Rheological Properties of Aqueous Solutions of Alkyl- and Oleyldimethylamine Oxides. Spinnability and Viscoelasticity

Kazuhiko Hashimoto and Toyoko Imae*

Department of Chemistry, Faculty of Science, Nagoya University, Nagoya 464, Japan

Received August 23, 1990. In Final Form: January 7, 1991

Spinnability and viscoelasticity have been measured for aqueous solutions of alkyl- and oleyldimethylamine oxides (C_nDAO, n = 14, 16, 18; ODAO) and sodium alginate. The aqueous solutions of C_{16}DAO at 35 °C presented the spinnability of "ductile failure" and the polymer-like viscoelasticity. This aspect is consistent with the existence of isolated rodlike micelles in dilute solutions and their entanglement at high surfactant concentrations. Similar behavior was also observed for aqueous solutions of ODAO with 0–2 M NaCl and C_{14}DAO with 0.2 M NaCl and various amounts of HCl. The aqueous solutions of C_{16}DAO at 20 °C and C_{18}DAO at 25 °C exhibited the spinnability of "cohesive fracture failure" and the gellike viscoelasticity. This behavior originates in the interacting platelike assemblies. The rheological properties of aqueuos solution of sodium alginate transferred gradually from dilute polymer-type to gel-type. This corresponds to the formation of linkage structure by interpolymer interaction in concentrated solutions.

Introduction

When a rod is immersed in a liquid and pulled up at a certain velocity, a liquid is stretched to form a thread. Such thread-forming property of a liquid, spinnability, has been investigated for some polymer solutions and related to the non-Newtonian viscosity and the viscoelasticity.[1-6] The spinnability has also been discovered for aqueous solutions of cationic surfactants with the aromatic counterions like salicylate,[7] which simultaneously exhibited strong viscoelasticity.[8-10]

We have recently measured the spinnability of aqueous solutions of tetradecyl- and hexadecyltrimethylammonium salicylates (C_{14}TASal, C_{16}TASal) with and without salt[11] and of water-soluble polymers.[12] The spinnability was classified into two types, D and C, after ductile failure (or capillary-ductile failure) and cohesive fracture failure, respectively.[13] The type D spinnability occurred from more viscous response and the type C spinnability corresponded to more elastic response. On the other hand, three types of viscoelasticities were observed in aqueous solutions of C_{14}TASal and C_{16}TASal with and without salt.[14] Those were gel-like, Maxwell-like, and polymer-like. It was supposed that pseudo network structure constituted by pseudolinkages and entanglement contacts was formed in spinnable and viscoelastic solutions.

The viscoelasticity was also reported for aqueous solutions of C_{14}DAO,[15] aqueous NaBr solutions of alkyltrimethylammonium bromides,[16,17] and mixed saline solutions of octadecylphenylalkoxysulfonates mixed with butan-2-ol.[18] Hoffmann et al.[15] have reported that the storage modulus of an aqueous solution of 1 M C_{14}DAO at 20 °C increased from 10^{-2} to 10 dyn cm^{-2} with an increase in frequency from 1 to 10^2 Hz.

In this work we report the spinnability and the viscoelasticity of aqueous solutions of C_nDAO (n = 14, 16, 18), ODAO, and sodium alginate, and discuss the rheological mechanism in those solutions.

Experimental Section

All samples were same as previously used.[12,19-22] Water was purified as usual.

The apparatus for the spinnability measurement and its procedure were described elsewhere in detail.[11,12] As a stainless steel rod of 5 mm in diameter was immersed in a solution and was driven up at a constant drawing velocity, v, a liquid was stretched to form a thread. The thread was broken off, when the rod reached at a certain height, drawing length, which was measured as the spinnability. The drawing length was extrapolated to zero immersed depth, since it changed linearly with the immersed depth of a rod.

The measurement of dynamic viscoelasticity was performed on a Rheology Engineering MR-3 rheometer. The isotropic solutions were measured by using the Couette coaxial cylinder cells composed of an outer cylinder with 4.00 cm inner diameter and an inner cylinder with 3.80 or 3.90 cm outer diameter and 1.00 cm height. A cell of cone and plate type with 3.20 cm diameter and 1.90° cone angle was utilized for the anisotropic solutions. The temperature of the cell chamber was kept within ±1 °C.

Results

The behavior of the intrinsic drawing length, L_0, at zero immersed depth against the drawing velocity was classified

(1) Jochims, J. *Kolloid-Z.* **1927**, *43*, 361.
(2) Erbring, H. *Kolloid-Beih.* **1936**, *44*, 171.
(3) Thiele, H.; Lamp, H. *Kolloid-Z.* **1952**, *129*, 25.
(4) Nakagawa, T. *Bull. Chem. Soc. Jpn.* **1952**, *25*, 88, 93.
(5) Inagaki, H. *J. Colloid Sci.* **1956**, *11*, 226.
(6) Akabane, H.; Nakahara, N. *Nihon Reoloji Gakkaishi* **1989**, *17*, 123.
(7) Gravsholt, S. *J. Colloid Interface Sci.* **1976**, *57*, 575.
(8) Kalus, J.; Hoffmann, H. *J. Chem. Phys.* **1987**, *87*, 714.
(9) Shikata, T.; Hirata, H.; Kotaka, T. *Langmuir* **1987**, *3*, 1081; **1988**, *4*, 354.
(10) Rehage, H.; Hoffmann, H. *J. Phys. Chem.* **1988**, *92*, 4712.
(11) Imae, T.; Hashimoto, K.; Ikeda, S. *Colloid Polym. Sci.* **1990**, *268*, 460.
(12) Hashimoto, K.; Imae, T. *Polym. J.* **1990**, *22*, 331.
(13) Ide, Y.; White, J. L. *J. Appl. Polym. Sci.* **1976**, *20*, 2511.
(14) Hashimoto, K.; Imae, T.; Nakazawa, K. *Colloid Polym. Sci.*, in press.
(15) Hoffmann, H.; Oetter, G.; Schwandner, B. *Prog. Colloid Polym. Sci.* **1987**, *73*, 95.
(16) Candau, S. J.; Hirsch, E.; Zana, R.; Adam, M. *J. Colloid Interface Sci.* **1988**, *122*, 430.
(17) Candau, S. J.; Hirsch, E.; Zana, R.; Delsanti, M. *Langmuir* **1989**, *5*, 1225.
(18) Greenhill-Hooper, M. J.; O'Sullivan, T. P.; Wheeler, P. A. *J. Colloid Interface Sci.* **1988**, *124*, 77, 88.
(19) Imae, T.; Ikeda, S. *J. Colloid Interface Sci.* **1984**, *98*, 363; *Colloid Polym. Sci.* **1984**, *262*, 497; *Colloid Polym. Sci.* **1985**, *263*, 756.
(20) Imae, T.; Kamiya, R.; Ikeda, S. *J. Colloid Interface Sci.* **1984**, *99*, 300.
(21) Abe, A.; Imae, T.; Shibuya, A.; Ikeda, S. *J. Surf. Sci. Technol.* **1988**, *4*, 67.
(22) Imae, T.; Sasaki, M.; Ikeda, S. *J. Colloid Interface Sci.* **1989**, *131*, 601.

0743-7463/91/2407-1734$02.50/0

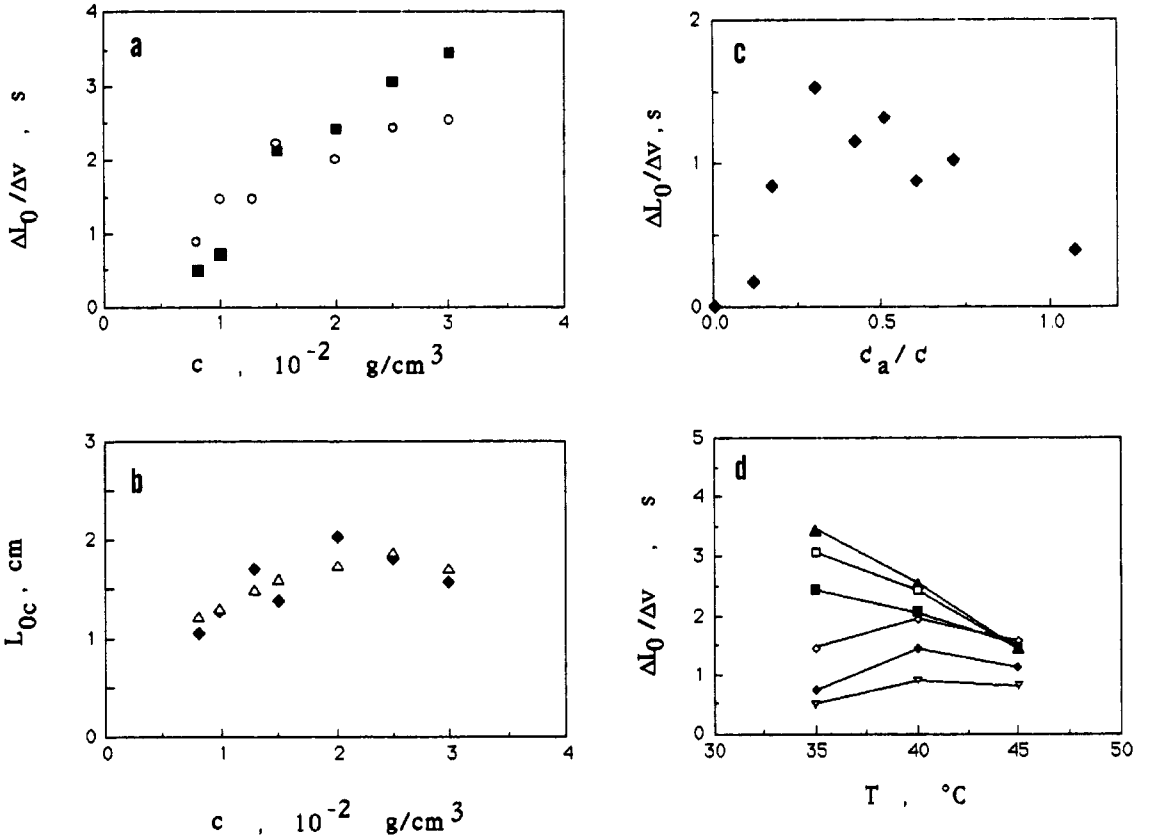

Figure 1. $\Delta L_0/\Delta v$ and L_{0c} values for aqueous solutions of C_nDAO: (a, b) $C_{16}DAO$ in water at (△) 20 °C; (◆) 25 °C; (■) 35 °C; (○) and 40 °C; (c) 5×10^{-2} g cm^{-3} $C_{14}DAO$ in 0.2 M NaCl at 25 °C; (d) $C_{16}DAO$ in water with surfactant concentration (10^{-2} g cm^{-3}) (▽) 0.8, (◆) 1.0, (◇) 1.5, (■) 2.0, (□) 2.5, and (▲) 3.0.

into two types; (1) the L_0 values increased linearly with the drawing velocity and (2) the L_0 values decreased with the drawing velocity or were independent of it. The former is called "type D" and the latter "type C".[11,12] The former was characterized by the slope, $\tan \alpha \equiv \Delta L_0/\Delta v$, of the straight line on the proportionality of the L_0 value against drawing velocity and the latter by L_{0c}, which is the L_0 value at high velocity or the constant L_0 value.

Type C spinnability was observed for aqueous solutions of $C_{16}DAO$ at 20 and 25 °C. As seen in Figure 1b, the L_{0c} values had a maximum at a surfactant concentration, c, of 2×10^{-2} g cm^{-3} but were independent of the temperature. Type D spinnability was observed for aqueous solutions of $C_{16}DAO$ at 35, 40, and 45 °C. The $\Delta L_0/\Delta v$ values are plotted as a function of the surfactant concentration in Figure 1a. The $\Delta L_0/\Delta v$ values increased with the surfactant concentration. The increase was sharp below 2×10^{-2} g cm^{-3} and gradual above it. As seen in Figure 1d, the $\Delta L_0/\Delta v$ values for solutions below 2×10^{-2} g cm^{-3} were highest at 40 °C but those above 2×10^{-2} g cm^{-3} decreased with increasing the temperature.

The aqueous solutions of $C_{14}DAO$ did not present spinnability even in the presence of 0.2 M NaCl. However, when HCl was added to them, type D spinnability was observed. Figure 1c shows the $\Delta L_0/\Delta v$ values at various C_a/C ratios for 0.2 M NaCl solutions of $C_{14}DAO$ of 5×10^{-2} g cm^{-3}, where C and C_a are the mole concentrations of $C_{14}DAO$ and HCl, respectively. With increasing HCl concentration, the $\Delta L_0/\Delta v$ values increased sharply initially and decreased gradually through the maximum at $C_A/C \approx 0.3$. Spinnability was maintained even in $C_a/C \approx 1.0$.

Only type D spinnability was observable for aqueous solutions of ODAO with and without NaCl. It can be seen in Figure 2a that, while the $\Delta L_0/\Delta v$ values at 35 °C for aqueous solutions of ODAO without salt were independent of the surfactant concentration, those at 25 °C increased with the initial increase of surfactant concentration but decreased slightly at high surfactant concentration. The $\Delta L_0/\Delta v$ values at 15 °C increased remarkably above 0.5×10^{-2} g cm^{-3}, below which there was no spinnability. The $\Delta L_0/\Delta v$ values at low surfactant concentrations increased with the rise of temperature from 15 to 35 °C, as shown in Figure 2c. The maximum $\Delta L_0/\Delta v$ values were seen at 35 °C for solutions of medium surfactant concentrations, and $\Delta L_0/\Delta v$ values at high surfactant concentrations decreased with temperature.

Spinnability of aqueous solutions of ODAO of 0.9×10^{-2} g cm^{-3} was measured in the presence of NaCl. As seen in Figure 2b, $\Delta L_0/\Delta v$ values scarcely depended on NaCl concentration, C_s, below 0.1 M but increased above 0.1 M.

The absolute complex viscosity, $|\eta^*|$, the storage modulus, G', and the loss modulus, G'', of aqueous solutions of $C_{16}DAO$ at 20 and 35 °C are drawn in Figures 3 and 4 as a function of angular frequency, ω. All of these increased as the surfactant concentration increased. The $|\eta^*|$ values decreased with an increase in ω values at 20 °C but were constant at low frequency at 35 °C.

Both G' and G'' values at 20 °C increased slowly with frequency, and the magnitude of the G'' values was slightly larger than that of G' values. This kind of viscoelasticity is a characteristic of the gel solutions of cross-linked polymers.[23] The G' and G'' values were distinct below 10^{-2} g cm^{-3} and above 2×10^{-2} g cm^{-3}. At each region, the concentration dependence of the G' and G'' values was

(23) Lodge, A. S. *Elastic Liquids*; Academic Press: New York, 1964. Ferry, J. D. *Viscoelastic Properties of Polymers*, 3rd ed.; Wiley: New York, 1980.

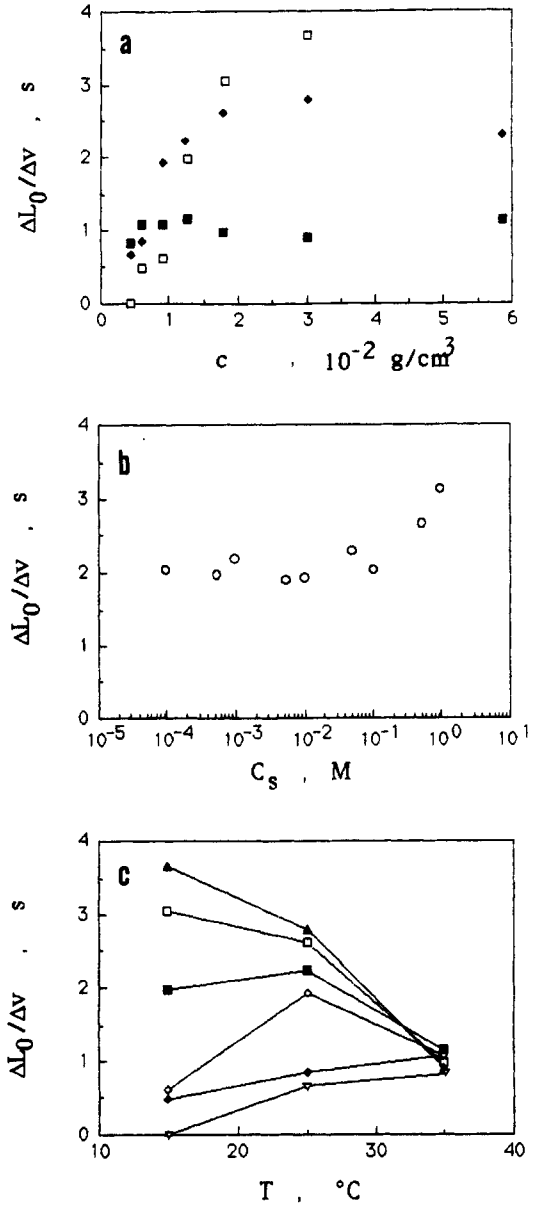

Figure 2. $\Delta L_0/\Delta v$ values for aqueous solutions of ODAO: (a) in water at (□) 15 °C, (◆) 25 °C, and (■) 35 °C; (b) of 0.9×10^{-2} g cm^{-3} in aqueous NaCl solutions at 25 °C; (c) in water with surfactant concentrations (10^{-2} g cm^{-3}) (▽) 0.6, (◆) 0.9, (◇) 1.3, (■) 1.8, (□) 3.0, and (▲) 6.0.

slight. The G' and G'' values at 35 °C increased sharply with the frequency. There was a small peak in a G''–ω plot for a solution of 3×10^{-2} g cm^{-3} but not for dilute solutions. This kind of viscoelasticity is often observed in polymer solutions.[23]

Figure 5 shows the G''–G' plot for aqueous solutions of C_{16}DAO at 35 °C. Although the plots for dilute solutions deviated from a semicircle, the plot for a solution of 3×10^{-2} g cm^{-3} was almost semicircular. From the frequency value giving rise to the maximum of a semicircle, relaxation time could be calculated as 0.3 s for a solution of 3×10^{-2} g cm^{-3} by the relation

$$\tau = 1/\omega_{max} \quad (1)$$

As seen in Figure 6, the $|\eta^*|$ values for aqueous solutions of C_{18}DAO at 25 °C decreased gradually with the frequency and did not reach a constant value even at low frequency. The frequency dependence of G' and G'' was small but the G'' values were larger than that of G'. The $|\eta^*|$, G', and G'' values increased with the surfactant concentration.

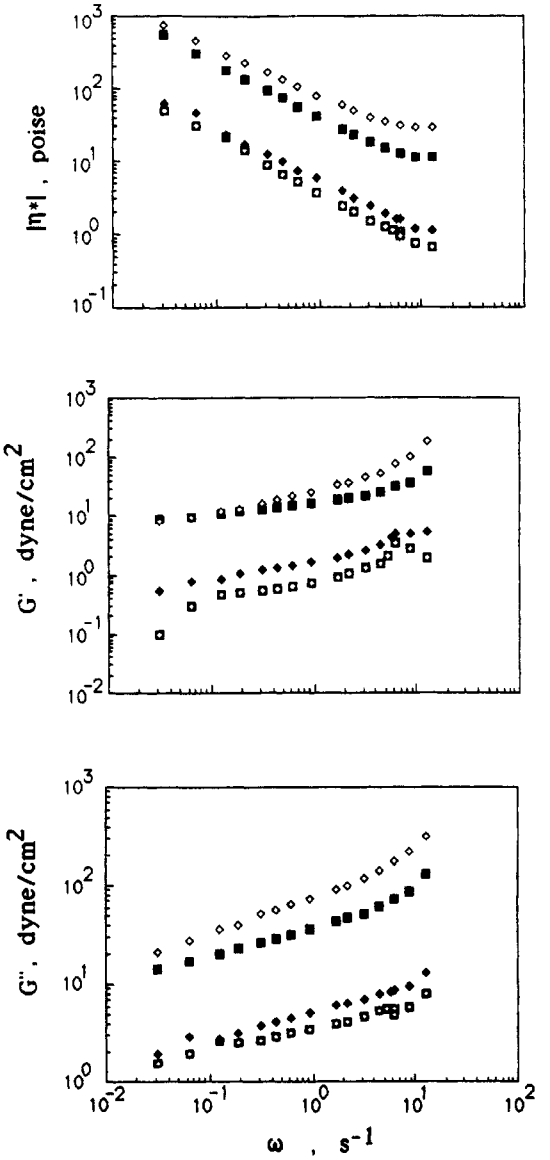

Figure 3. $|\eta^*|$, G', and G'' values for aqueous solutions of C_{16}DAO at 20 °C and surfactant concentrations (10^{-2} g cm^{-3}) of (□) 0.5, (◆) 1.0, (■) 2.0, and (◇) 3.0.

The concentration gap in G' and G'' plots was observed between 3×10^{-2} and 5×10^{-2} g cm^{-3}. The behavior was very similar to that of aqueous solutions of C_{16}DAO at 20 °C.

Figure 7 represents the $|\eta^*|$, G', and G'' values for aqueous solutions of ODAO without salt at 25 °C. Those increased with increasing surfactant concentration. The $|\eta^*|$ values were independent of the initial frequency increase but decreased at high frequency. As the frequency increased, the G' and G'' values increased, except that the G'' values had a small maximum for solutions of 3×10^{-2} and 6×10^{-2} g cm^{-3}. The G''–G' plot for these two solutions presented a semicircular feature. The evaluated relaxation time was 0.3 and 0.9 s, respectively. The temperature dependence of $|\eta^*|$, G', and G'' was measured at 15–35 °C for aqueous solutions of ODAO of 0.9×10^{-2} g cm^{-3} but the difference was small. The viscoelastic behavior of aqueous solutions of ODAO was similar to that of aqueous solutions of C_{16}DAO at 35 °C.

The viscoelasticity of aqueous solutions of ODAO of 0.9×10^{-2} g cm^{-3} was measured at various NaCl concentrations at 25 °C and the results are shown in Figure 8. The $|\eta^*|$, G', and G'' values were only slightly dependent on NaCl concentration below 0.1 M but increased with NaCl

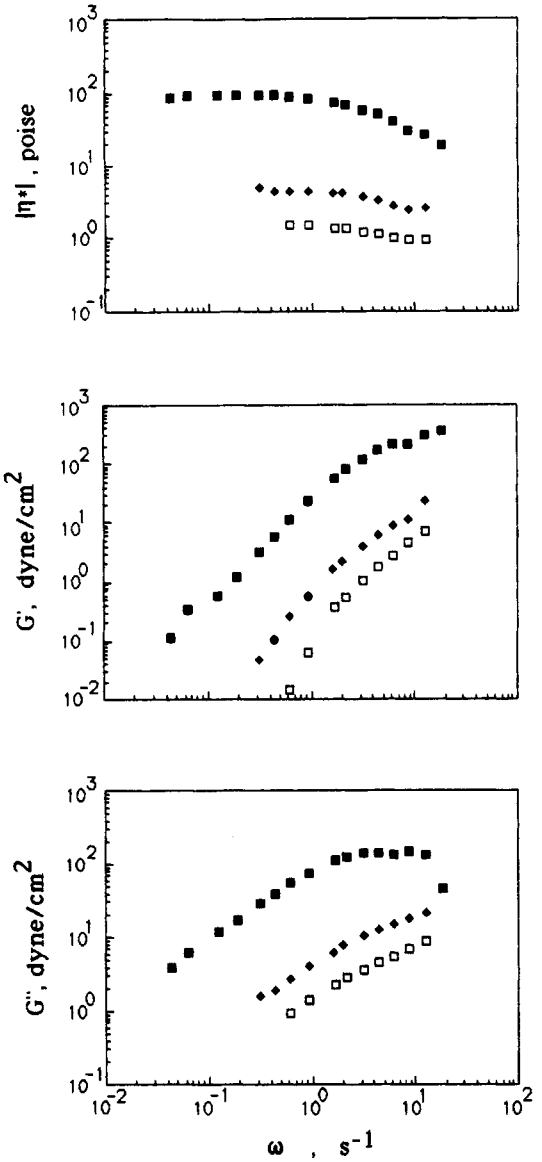

Figure 4. $|\eta^*|$, G', and G'' values for aqueous solutions of C_{16}DAO at 35 °C and surfactant concentrations (10^{-2} g cm^{-3}) of (□) 1.0, (◆) 2.0, and (■) 3.0.

concentration above 0.1 M. The plateaus of $|\eta^*|$ and G' appeared at low and high frequencies, respectively, for solutions with high NaCl concentration. The dynamic modulus of the plateau in a G'–ω plot, G_N, was 22 dyn cm^{-2}. The G'' values increased through a small peak with an increase in angular frequency, when NaCl concentration was higher than 0.5 M. The peak position shifted to lower frequency region with NaCl concentration. Correspondingly, the relaxation time lengthened from 0.3 s at 0.5 M NaCl to 0.7 s at 2 M NaCl.

The viscoelasticity of aqueous solutions of sodium alginate was measured at various polymer concentrations at 25 °C and the results are given in Figure 9. With increasing sodium alginate concentration, the $|\eta^*|$, G', and G'' values increased. $|\eta^*|$ values were almost independent of the frequency at low sodium alginate concentration and decreased slighly with increasing the frequency at high sodium alginate concentration. G' and G'' values increased monotonically with the frequency, and the form of the log G''–log ω plot was similar with that of the log G'–log ω plot. When the concentration was increased, the frequency dependence decreased; that is, the slopes of the log G'–log ω and log G''–log ω plots decreased, indicating enhancement of the interaction between polymer chains.

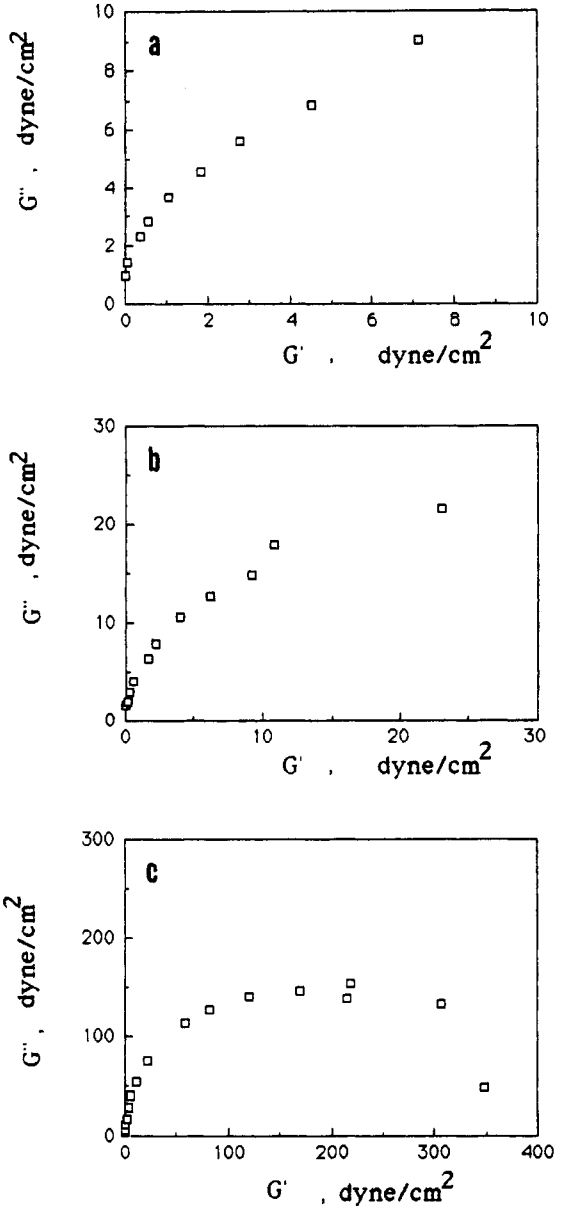

Figure 5. G''–G' plots for aqueous solutions of C_{16}DAO at 35 °C and surfactant concentrations (10^{-2} g cm^{-3}) of (a) 1.0, (b) 2.0, and (c) 3.0.

The constant $|\eta^*|$ value at low frequency or the $|\eta^*|$ value at lowest frequency examined here can be equated to the η_0 value by

$$\eta_0 \equiv \lim_{D\to 0} \eta(D) \equiv \lim_{\omega\to 0} |\eta^*(\omega)| \qquad (2)$$

according to the Cox–Merz relation,[23,24] where η_0 is the steady-state viscosity and D is the shear rate. The η_0 values were plotted in Figures 10 and 11 as a function of surfactant or polymer concentration, c, for aqueous solutions of C_{16}DAO, C_{18}DAO, ODAO, and sodium alginate. The linear relation of η_0 and c was obtained in a double-logarithmic scale. On the other hand, as seen in Figure 11, the η_0 values at 25 °C for aqueous NaCl solutions of ODAO of 0.9×10^{-2} g cm^{-3} were almost constant at low NaCl concentrations but increased remarkably above 0.1 M NaCl.

Discussion

The spinnability of aqueous solutions of alkyl- and oleyldimethylamine oxides and sodium alginate could be

(24) Cox, W. P.; Merz, E. H. *J. Polym. Sci.* **1958**, *28*, 619.

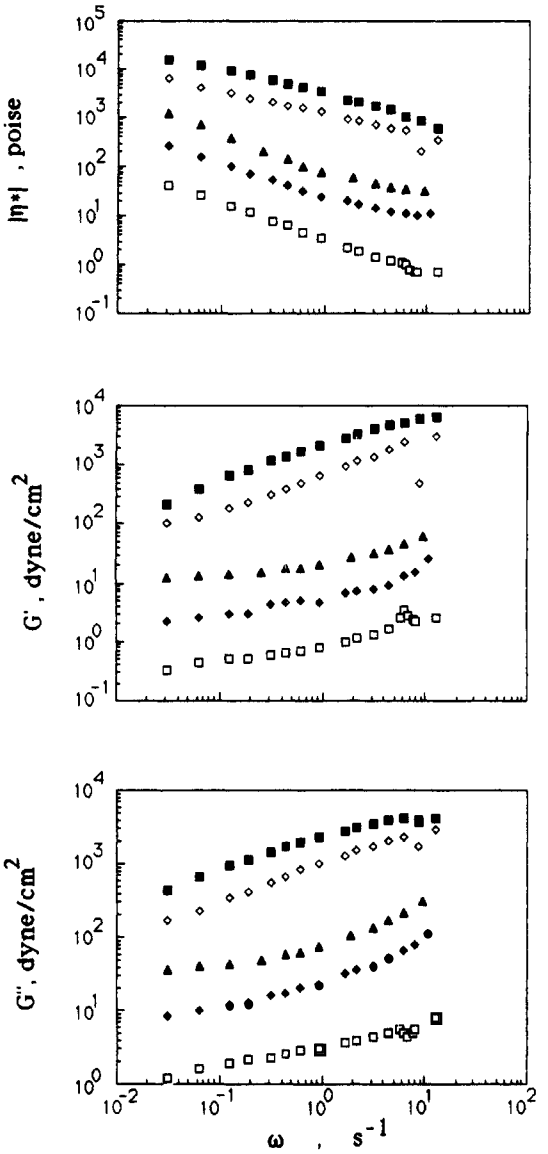

Figure 6. $|\eta^*|$, G', and G'' values for aqueous solutions of C_{18}-DAO at 25 °C and surfactant concentrations (10^{-2} g cm^{-3}) of (□) 0.5, (◆) 1.0, (▲) 3.0, (◇) 5.0, and (■) 10.0.

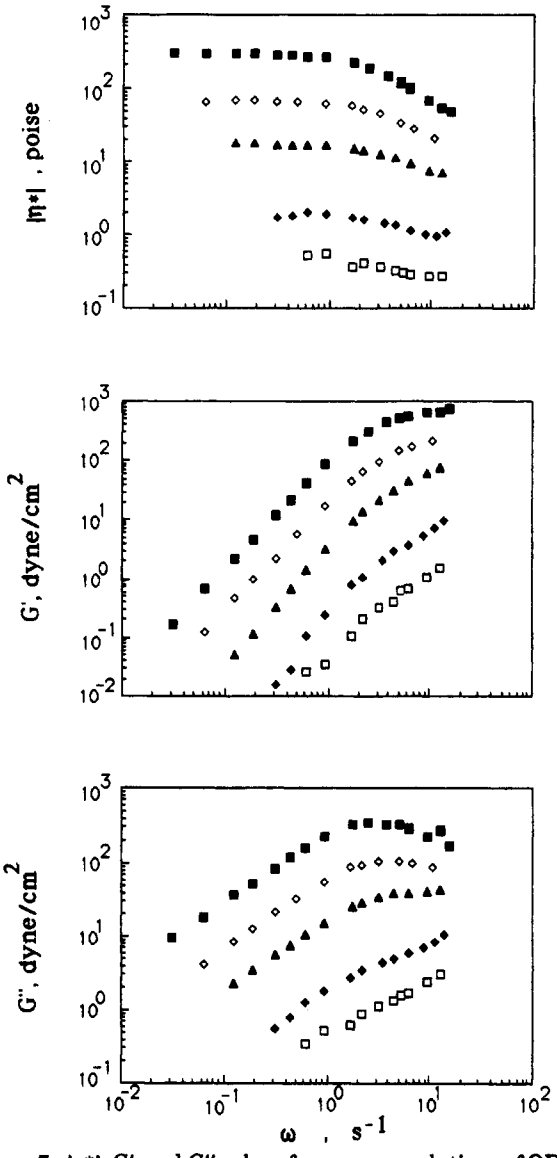

Figure 7. $|\eta^*|$, G', and G'' values for aqueous solutions of ODAO at 25 °C and surfactant concentrations (10^{-2} g cm^{-3}) of (□) 0.45, (◆) 0.9, (▲) 1.8, (◇) 3.0, and (■) 6.0.

divided into two types, D and C, from a relation of the intrinsic drawing length to the drawing velocity. The intrinsic drawing length in type D spinnability was proportional to the drawing velocity and that in type C spinnability decreased with the drawing velocity or was independent of it. Type D spinnability was observed for aqueous solutions of C_{14}DAO in the presence of NaCl and HCl at 25 °C, C_{16}DAO at 35–45 °C, and ODAO with 0–1 M NaCl at 15–35 °C. Aqueous solutions of C_{16}DAO at 20 and 25 °C presented type C spinnability.

The frequency dependence of the viscoelasticity may also be classified into two groups. In the polymer-type viscoelasticity, the G' and G'' values increased monotonically with the angular frequency at low surfactant (or polymer) concentration and/or low NaCl concentration. On the other hand, at high surfactant concentration and/or high NaCl concentration, whereas the G' and G'' values initially increased linearly with the frequency, the G' values reached a constant value at high frequency and G'' values had a small peak. Polymer-type viscoelasticity was found in aqueous solutions of C_{16}DAO at 35 °C, ODAO, and sodium alignate at low polymer concentration. The aqueous solutions of ODAO with high NaCl concentration presented the G'' curves increasing through a small maximum.

The aqueous solutions of C_{16}DAO at 20 °C, C_{18}DAO at 25 °C, and sodium alginate at high polymer concentration exhibited the viscoelastic feature where both G' and G'' values increased slightly with increasing angular frequency. This type of viscoelasticity is gellike.

In dilute solutions of polymers and even in the melts or concentrated solutions of short polymers, a polymer chain such as represented by a Rouse model can be constituted by many segments (beads) and Gaussial chains (springs), and the relaxation spectra of the viscoelasticity are determined by the cooperativity of the segment motion without the intra- and interpolymer interactions. Then the energy dispersion by the viscosity overcomes the energy storage by the elasticity. The G' and G'' values increase with a slope of 2 and unity, respectively, when the G' and G'' values are plotted as a function of angular frequency in a double-logarithmic scale.

The viscoelasticity of entangled polymers, which is observed in the concentrated solutions or melts, is characterized by the flow (terminal), rubbery, transition, and glassy regions. As the angular frequency increases, the G'

values increase with a slope of 2 in the flow region, reach a constant value in the rubbery region, and then increase again in order to reach the glassy region through the transition region. The relaxation times are observed at the flow and transition regions. The G'' curves have an initial slope of unity and exhibit two maxima, corresponding to two relaxation times.

When a strong three-dimensional structure with cross-links between polymers is formed over wide distances, gel-type viscoelasticity is observed, and it has long lifetime processes. The structure is stronger than that formed by solution of polymers without cross-linkages, and the motion of the long lifetime processes only relaxes slowly. An extreme case is an ideal elastic solid like a gel linked by covalent bonds or crystallized polymers.

The types of spinnability and viscoelasticity for some solutions examined in the present work are listed in Table I. Table I also includes results from the literature,[11,12,14,25] and values of the initial slope, x and y, in log G'–log ω and log η_0–log c plots written as

$$G' \sim \omega^x \tag{3}$$

and

$$\eta_0 \sim c^y \tag{4}$$

The shapes of surfactant assembly in solutions[14,19,20,26,27] are described in the last column in Table I. As seen in Table I, type D spinnability can be related to the dilute and/or entangled polymer-type viscoelasticity and the type C spinnability is gel-type.

The viscoelastic fluid must behave elastically in a certain frequency and time region and as viscous fluid in the other frequency and time region. Then the type C or D spinnability is observed depending upon whether the relaxation time is longer or shorter than the time constant of the drawing examined. As a result, when the conditions conform to viscous type D behavior, the frequency dependence of G' is large. On the other hand, the viscoelastic solid (gel) must respond elastically over a wide frequency region. Therefore the elastic type C spinnability is always presented, even at any drawing velocity, and the frequency dependence of G' is small. This aspect is obvious from the values of initial slope in a plot of log G' as a function of log ω as listed in Table I; the solutions in type D had a slope of 1.7–2.0, as was expected, and those in type C exhibited a slope below unity.

Type D spinnability for C_{14}DAO in 0.2 M NaCl increased with an initial increase in C_a/C value, and the $\Delta L_0/\Delta v$ values decreased above C_a/C values of 0.3. When a moderate amount of HCl is added, charged C_{14}DAO molecules make pairs with noncharged molecules and the growing and entanglement of rodlike micelles are induced, resulting in the strengthening of the type D spinnability. At high C_a/C values where the charged molecules increase further, the size of micelles decreases by the electrostatic repulsion between charged surfactants in a micelle, and the type D spinnability weakens.

The viscoelasticity of dilute aqueous solutions of C_{16}DAO at 35 °C and ODAO at 25 °C was similar to the viscoelastic behavior of dilute nonlinked polymer solutions, and that of concentrated solutions was like that of entangled polymer solutions. This aspect is consistent with rodlike micelles being formed in dilute solutions of such surfactants and entangling each other at high surfactant concentrations.[19,26]

(25) Sasaki, M. M.S. Thesis, Nagoya University, 1989.
(26) Imae, T. Submitted for publication.
(27) Imae, T.; Trend, B. *J. Colloid Interface Sci.*, in press.

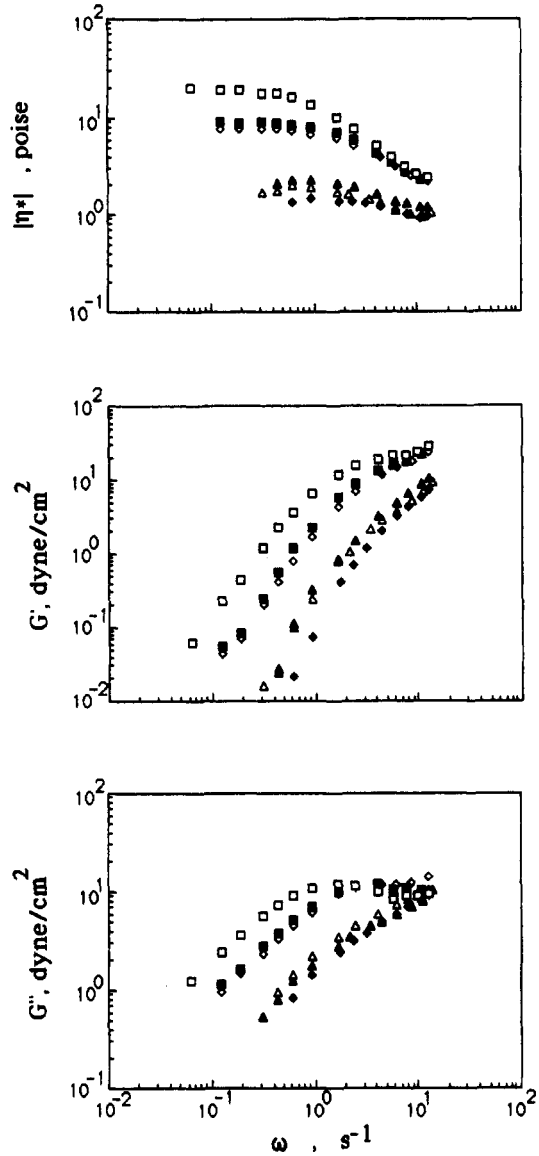

Figure 8. $|\eta^*|$, G', and G'' values for aqueous NaCl solutions of 0.9×10^{-2} g cm^{-3} ODAO at 25 °C and NaCl concentrations (M) of (◆) 0, (△) 0.0001, (▲) 0.1, (◇) 0.5, (■) 1.0, and (□) 2.0.

With an increase in temperature, the micellar molecular weight of nonionic surfactants generally increases, but the intermicellar interaction decreases. These two opposing effects give rise to the different behavior in terms of the temperature dependence of type D spinnability at low and high concentrations of C_{16}DAO and ODAO. At low concentrations the increase in micellar size due to the temperature effect is dominant, and $\Delta L_0/\Delta v$ values increase slightly with the temperature. At high concentrations, since the rodlike micelles are very long at all temperatures, the decrease in the micellar interaction is dominant at high temperature and the $\Delta L_0/\Delta v$ values decrease with the temperature, although the viscoelasticity of aqueous solutions of ODAO is scarcely affected by the temperature.

When NaCl is added to aqueous solutions of ODAO, rodlike micelles of ODAO grow in size and the entanglement between rodlike micelles is enhanced, but the intermicellar interaction is shielded.[19] The former increases the rheological behavior but the latter weakens it. The spinnability and the viscoelasticity are not strongly affected by the addition of NaCl concentration below 0.5 M as a result of the compensation between these two opposing effects. The micellar growing and entanglement

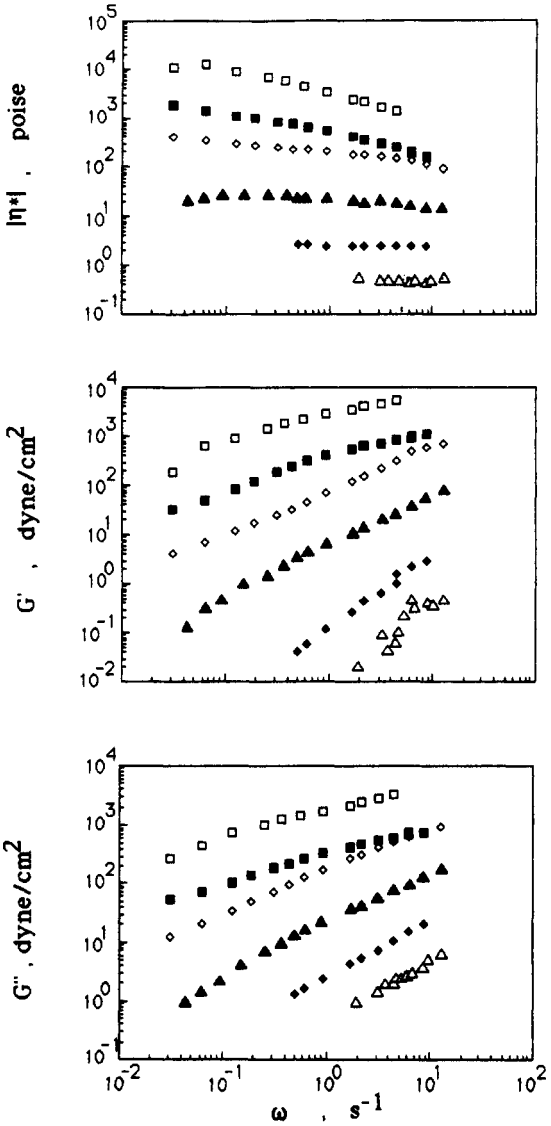

Figure 9. $|\eta^*|$, G', and G'' values for aqueous solutions of sodium alginate at 25 °C and polymer concentrations (10^{-2} g cm^{-3}) of (△) 0.5, (◆) 1.0, (▲) 2.0, (◇) 5.0, (■) 7.0, and (□) 10.0.

effects are most noted above 0.5 M NaCl and the spinnability increases. Simultaneously, the transition of the viscoelasticity from a dilute polymer-like behavior to an entangled polymer-like one is induced by the addition of 0.1–0.5 M NaCl.

A video-enhanced microscopic observation was carried out for aqueous solutions of C_{16}DAO and C_{18}DAO at room temperature, and platelike assemblies and their piles were observed.[27] Such solutions exhibited rheological behavior which was different to that of aqueous micellar solutions: the G' and G'' values depended slightly on the frequency, and the spinnability of platelike assembly solutions of C_{16}DAO at 20 and 25 °C was in type C, indicating the gellike viscoelasticity. Platelike assembly solutions of C_{16}DAO and C_{18}DAO of 0.3–2 wt % showed iridescence and those above 2 wt % were turbid.[22] The corresponding rheological distinction between two concentration regimes was observed as the maximum of L_{0c} values at 2×10^{-2} g cm^{-3} and the concentration gap of $|\eta^*|$, G', and G'' values between 1×10^{-2} and 2×10^{-2} g cm^{-3} for platelike assembly solutions of C_{16}DAO.

Type C spinnability is related to the elastic character and the gellike viscoelasticity responds elastically even at low frequency. Then a long range structure as well as gel exists in the platelike assembly solution, and such a

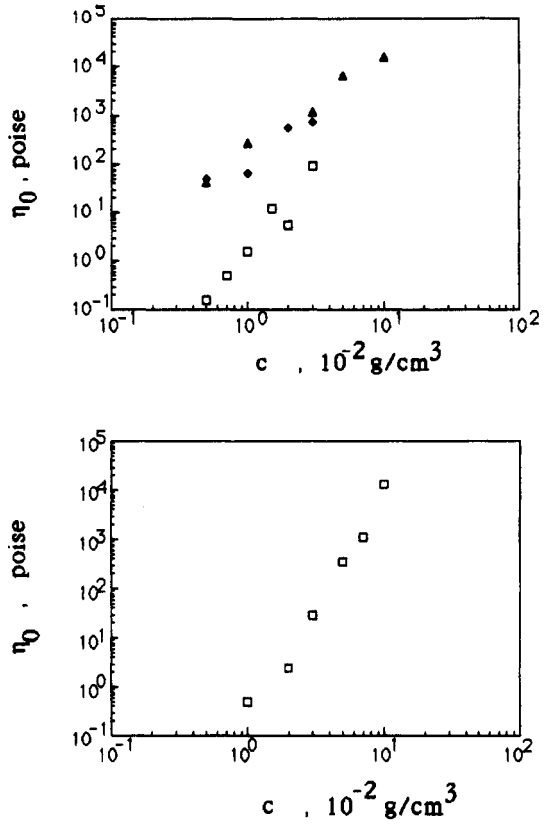

Figure 10. η_0 values for aqueous solutions of C_nDAO and sodium alginate: upper, (◆) C_{16}DAO at 20 °C, (□) C_{16}DAO at 35 °C, (▲) C_{18}DAO at 25 °C; lower, sodium alignate at 25 °C.

structure has a longer relaxation time than the experimental time scale. Therefore, when the rod is driven up on the spinnability experiment, the stretched solution produces a large stress. Above a certain stress, the pulling-back into the solution reservoir by the elastic force is stronger than the cohesion of the solution. Then the thread breaks. The relaxation of the elasticity by the flow (or viscosity) may not act there.

Viscoelasticity has been investigated for dispersions of latex.[28-32] It was indicated that latex particles with low surface charge in an aqueous polyacrylamide solution formed aggregates and the aggregate structure induced plateau regions at low frequency in frequency-dependent curves of G' and G''.[28] On the other hand, latex particles with high surface charge did not produce the aggregate structures, and these suspensions behaved like Newtonian liquids. Platelike assemblies of C_nDAO interacting in water can form a pilelike structure and such structures may induce dynamic viscoelasticity with the plateau regions at low frequency in G' and G'' plots in a similar manner to suspensions of latex particles with low surface charge.

Water-soluble polymers can form the network structure linked by the interpolymer interaction in an aqueous solution; they may associate with each other through counterions in the medium and form helical chain sections which form the junction zones by their lateral aggregation.[33]

(28) Matsumoto, T.; Yamamoto, O.; Onogi, S. *J. Rheol.* **1980**, *24*, 379.
(29) Buscall, R.; Goodwin, J. W.; Hawkins, M. W.; Ottewill, R. H. *J. Chem. Soc., Faraday Trans.* **1982**, *78*, 2873, 2889.
(30) Goodwin, J. W.; Gregory, T.; Miles, J. A.; Warren, B. C. H. *J. Colloid Interface Sci.* **1984**, *97*, 488.
(31) Goodwin, J. W.; Hughes, R. W.; Partridge, S. J.; Zukoski, S. J. *J. Chem. Phys.* **1986**, *85*, 559.
(32) Nagele, G.; Klein, R.; Frisch, H. L. *Colloid Polym. Sci.* **1988**, *266*, 437.

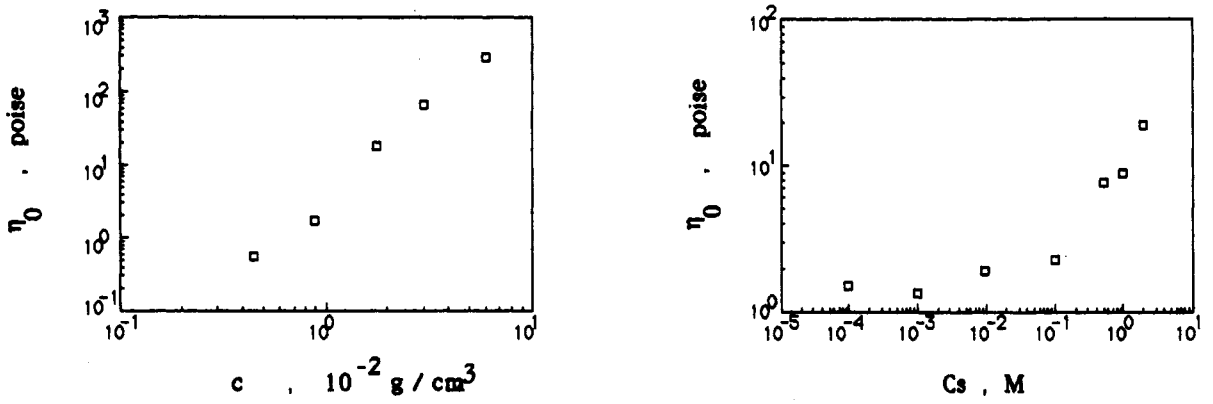

Figure 11. η_0 values for aqueous solutions of ODAO at 25 °C: left, in water; right, 0.9 × 10^{-2} g cm^{-3} in aqueous NaCl solution.

Table I. Rheological Characteristics of Aqueous Solutions of Surfactants and Polymer

	solvent	T, °C	c, 10^{-2} g cm^{-3}	x	viscoelasticity	spinnability	y	assembly shape[d]
C_{14}DAO	0.2 M NaCl, C_s/C = 0–1	25	5		polymer[b]	D		rodlike micelle
C_{16}DAO	water	20	1–3	0.2–0.3	gel	C	1.31	platelike assembly
		35	1–3	1.7–2.0	polymer	D	3.52	rodlike micelle
C_{18}DAO	water	25	0.5–3		gel		1.96	platelike assembly
ODAO	water	25	0.45–6	1.8–2.0	polymer	D	2.53	rodlike micelle
	0–2 M NaCl	25	0.9		polymer	D		rodlike micelle
sodium alginate	water	25	1	1.8	polymer			
		25	2–5	0.9–1.5	polymer + gel	D[c]	4.48	
		25	7, 10	0.5–0.7	gel	C[c]		
C_{14}TASal[a]	water	25	0.8–3.2		Maxwell + gel	D	3.20	linked short rod micelle
		25	10		gel	C		

[a] From refs 11 and 14. [b] From ref 25. [c] From ref 12. [d] From refs 14, 19, 20, 26, and 27.

Sodium alginate makes egg-box type double strands mediated by divalent metal ions like Ca^{2+}, and lateral aggregation between double strands is subsequently formed.[33,34] The interpolymer association through ordered junction zones is even induced by alkaline-metal ions like Na^+.[35] Then the linkages between polymers are stronger than the entanglement contact and exist for long time. Such high-order structure (linkage structure), which was strengthened by the interpolymer interaction, provided viscoelastic character to the solution in addition to viscous behavior.

It was confirmed in this work that the linkage structure of sodium alginate was constituted gradually with increasing polymer concentration, resulting in the gradual transition from polymer-type viscoelasticity to gel-type viscoelasticity. The formation of linkage structure by interpolymer interactions has also been demonstrated for aqueous solutions of sodium carboxymethylcellulose,[36] polyethylene oxide,[37] and thermoplastic elastomer.[38,39]

(33) Burchard, W. *Br. Polym. J.* **1985**, *17*, 154.
(34) Morris, E. R.; Rees, D. A.; Robinson, G.; Young, G. A. *J. Mol. Biol.* **1980**, *138*, 363. Morris, E. R.; Rees, D. A.; Thom, D.; Boyd, J. *Carbohydr. Res.* **1978**, *66*, 145.
(35) Seale, R.; Moris, E. R.; Rees, D. A. *Carbohydr. Res.* **1982**, *110*, 101.
(36) Rees, D. A. *Adv. Carbohydr. Chem. Biochem.* **1969**, *24*, 267.
(37) Sarkar, A.; Glrosh, K. *Kolloid Z. Z. Polym.* **1970**, *236*, 140.
(38) Stadler, R.; de Lucca Freitas, L. *Colloid Polym. Sci.* **1986**, *264*, 773.
(39) de Lucca Freitas, L.; Stadler, R. *Macromolecules* **1987**, *20*, 2478.